Ioffe Physico-Technical Institute, St. Petersburg, Russia

Interface-induced lateral anisotropy of semiconductor heterostructures

M.O. Nestoklon,

JASS 2004

Contents

- Introduction
- Zincblende semiconductors
- Interface-induced effects
- Lateral optical anisotropy: Experimental
- Tight-binding method
  - Basics
  - Optical properties in the tight-binding method
- Results of calculations
- Conclusion

Motivation

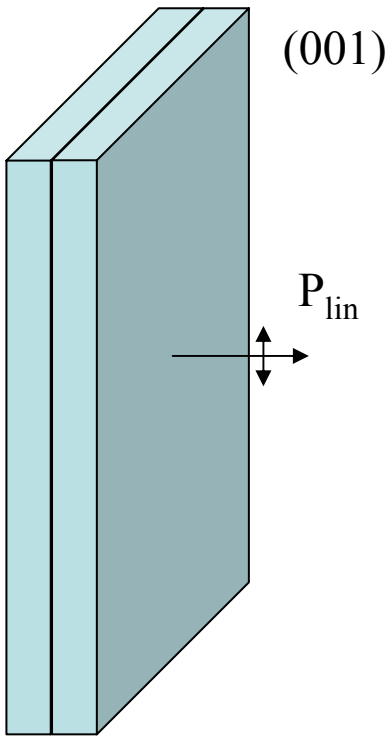

$$P_{\text{lin}} = \frac{I_x - I_y}{I_x + I_y}$$

The light, emitted in the (001) growth direction was found to be linearly polarized

This can not be explained by using the T_d symmetry of bulk compositional semiconductor

Zincblende semiconductors

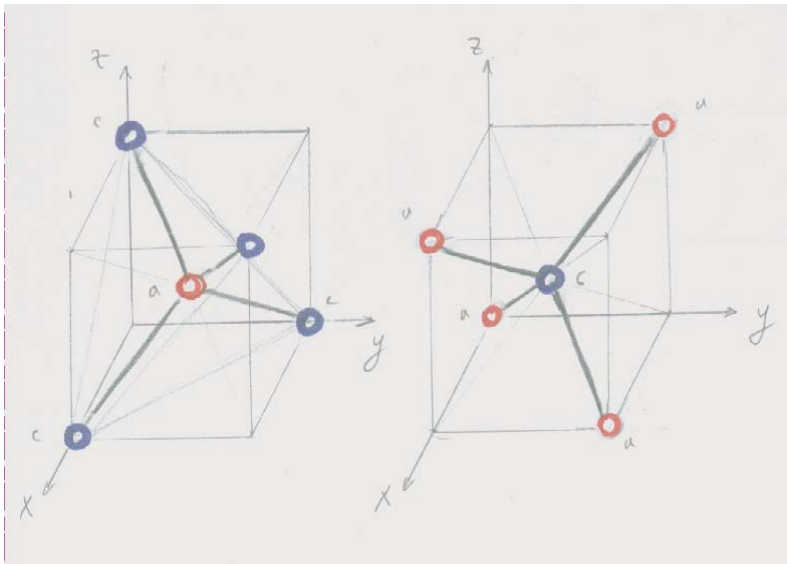

T_d symmetry determines bulk semiconductor bandstructure

However, we are interested in heterostructure properties.

An (001)-interface has the lower symmetry

Zincblende semiconductors

The point symmetry of a single (001)-grown interface is C_{2v}

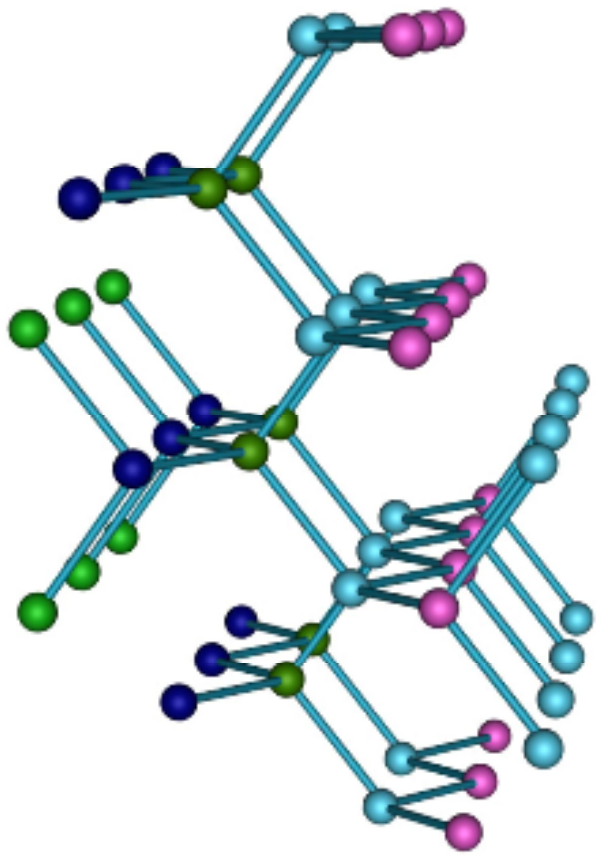

Envelope function approach

Electrons and holes with the effective mass

$$\left[-\frac{\hbar^2}{2m^*}\Delta + V(\boldsymbol{x})\right]\psi = E\psi$$

The Kane model takes into account complex band structure of the valence band and the wave function becomes a multi-component column.
The Hamiltonian is rather complicated…

Zincblende semiconductor bandstructure

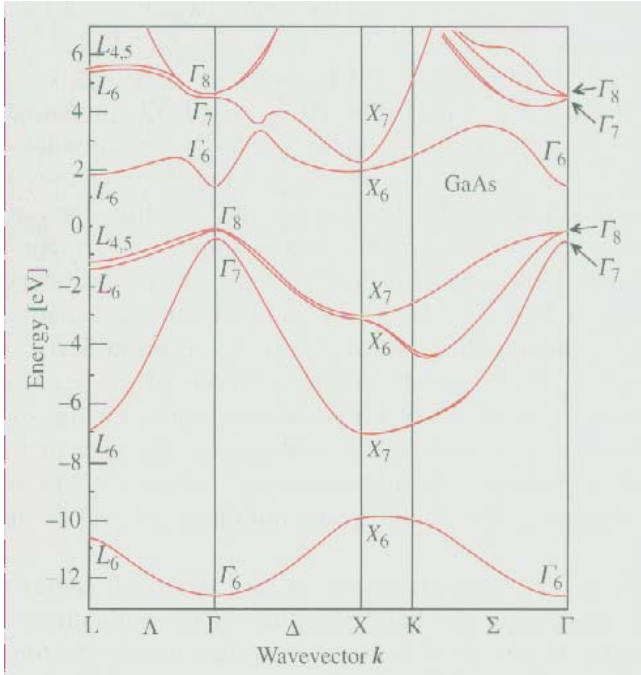

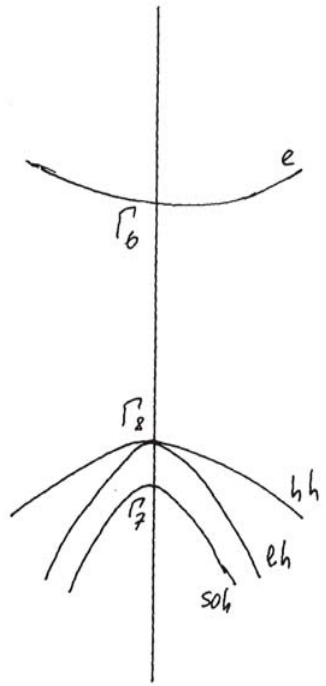

hh, lh holes have the total angular momentum ("spin") $J = \frac{3}{2}$

soh, e have spin $J = \frac{1}{2}$

hh spin projection $l = \pm\frac{3}{2}$

lh, soh, e spin projection $l = \pm\frac{1}{2}$

Rotational symmetry

If we have the rotational axis C_∞, we can define the angular momentum component ℓ as a quantum number

$\ell = 0, \pm1, \pm2, \pm3, \ldots$

$\ell = \pm1/2, \pm3/2, \ldots$

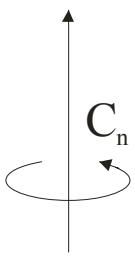

C_n has n spinor representations $D_l(c_n^k) = e^{\frac{2\pi i l}{n}k}$

The angular momentum can unambiguously be defined only for

$\ell = 0, \pm1, \pm2, \pm3, \ldots$

$\ell = \pm1/2, \pm3/2, \ldots$

$\| \quad -n/2 < \ell \leq n/2$

C_{2v} contains the second-order rotational axis C_2 and *does not* distinguish spins differing by 2

For the C_{2v} symmetry, states with the spin +1/2 and -3/2 are coupled in the Hamiltonian.

Crystal symmetry

As a result of the translational symmetry, the state of an electron in a crystal is characterized by the value of the wave vector **k** and, in accordance with the Bloch theorem,

$$\psi_{\boldsymbol{k}}(\boldsymbol{r}) = e^{i\boldsymbol{k}\cdot r} u_{\boldsymbol{k}}(\boldsymbol{r})$$

Let us remind that **k** is defined in the first Brillouin zone. We can add any vector from reciprocal lattice.

$$\boldsymbol{b}_1 = \frac{2\pi}{V}[\boldsymbol{a}_2 \times \boldsymbol{a}_3], \quad \boldsymbol{b}_2 = \frac{2\pi}{V}[\boldsymbol{a}_3 \times \boldsymbol{a}_1], \quad \boldsymbol{b}_3 = \frac{2\pi}{V}[\boldsymbol{a}_1 \times \boldsymbol{a}_2].$$

In the absence of translational symmetry the classification by **k** has no sense.

Examples

Γ-X coupling occurs due to translational symmetry breakdown

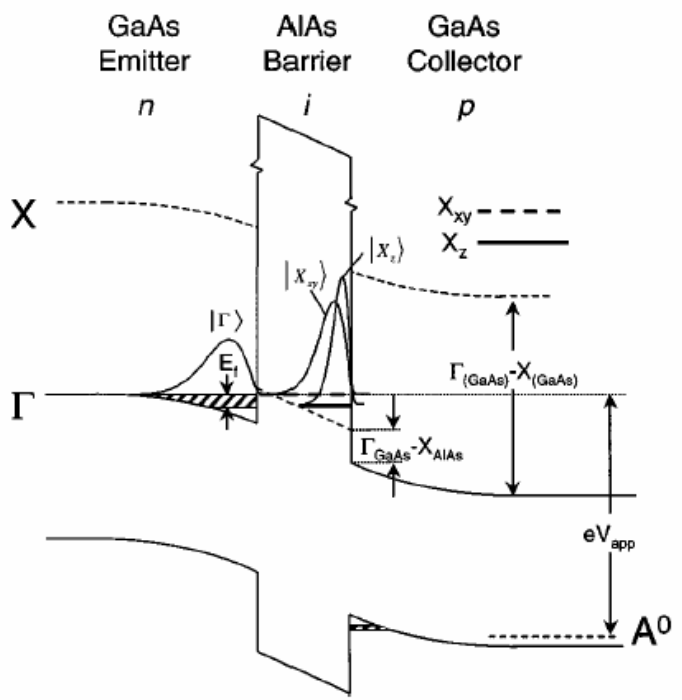

J. J. Finley et al, Phys. Rev. B, **58**, 10 619, (1998)

Schematic representation of the band structure of the p-i-n GaAs/AlAs/GaAs tunnel diode. The conduction-band minima at the Γ and X points of the Brillouin zone are shown by the full and dashed lines, respectively. The X point potential forms a quantum well within the AlAs barrier, with the Γ-X transfer process then taking place between the Γ-symmetry 2D emitter states and quasi-localized X states within the AlAs barrier.

hh-lh mixing

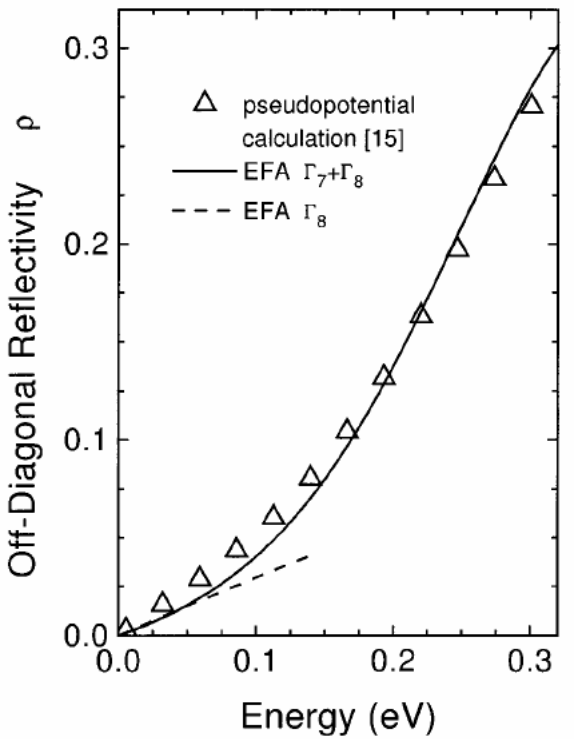

E.L. Ivchenko, A. Yu. Kaminski, U. Roessler, Phys. Rev. B **54**, 5852, (1996)

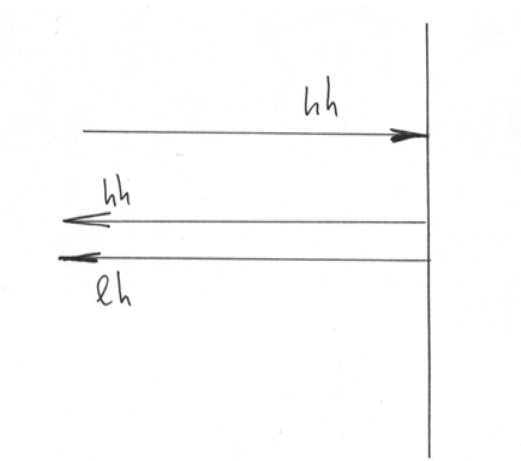

Type-I and -II heterostrucrures

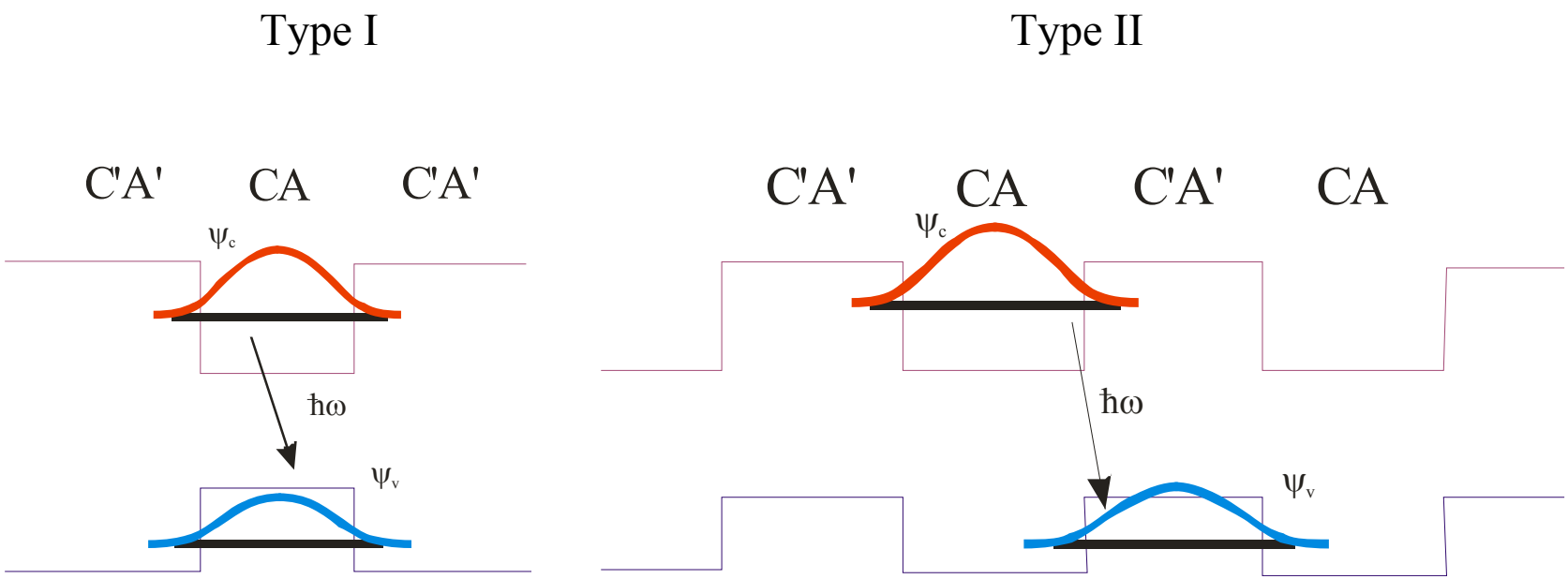

The main difference is that interband optical transition takes place only at the interface in type-II heterostructure when, in type-I case, it occurs within the whole CA layer

Lateral anisotropy

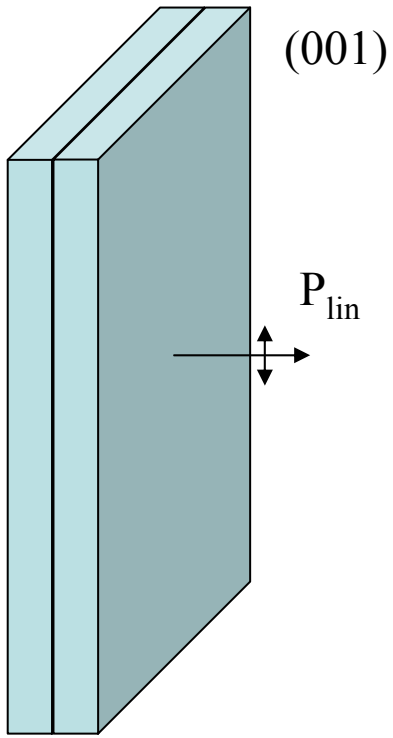

$$P_{\text{lin}} = \frac{I_x - I_y}{I_x + I_y}$$

type I $P_{\text{lin}} \sim 10 - 15\%$

type II $P_{\text{lin}} \sim 60 - 80\%$

Optical anisotropy in ZnSe/BeTe

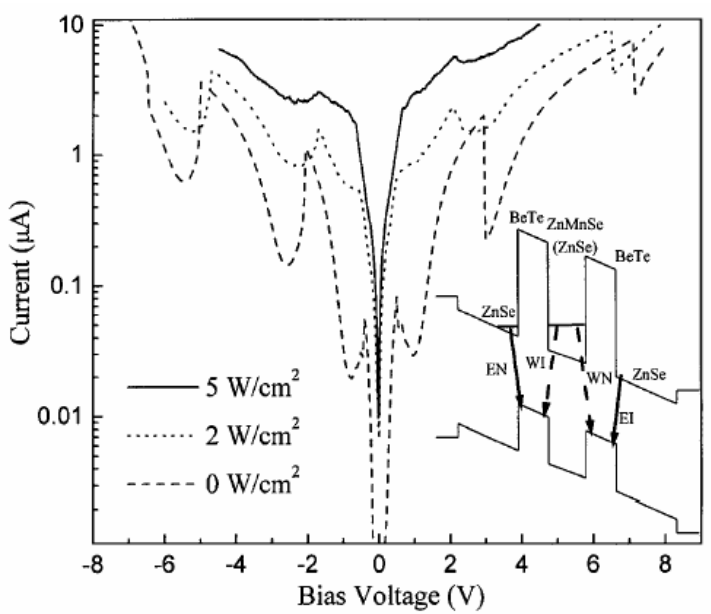

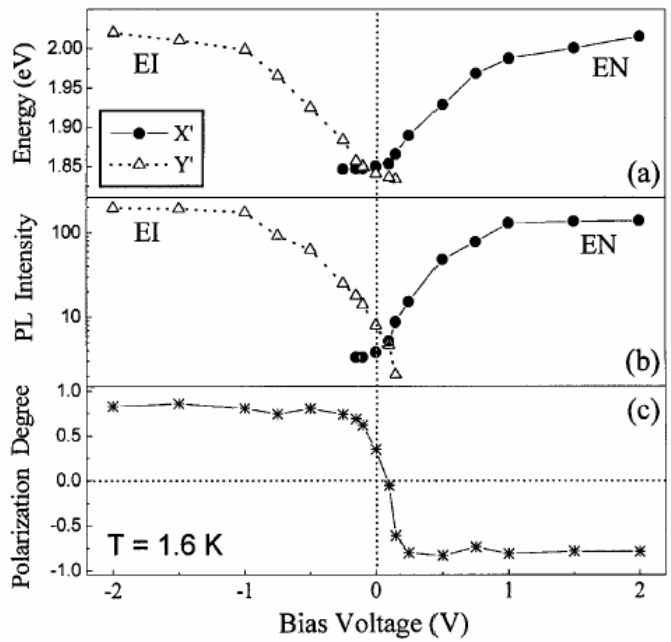

A.V. Platonov, V. P. Kochereshko,
E. L. Ivchenko et al., Phys. Rev. Lett. **83**, 3546 (1999)

Optical anisotropy in the InAs/AlSb

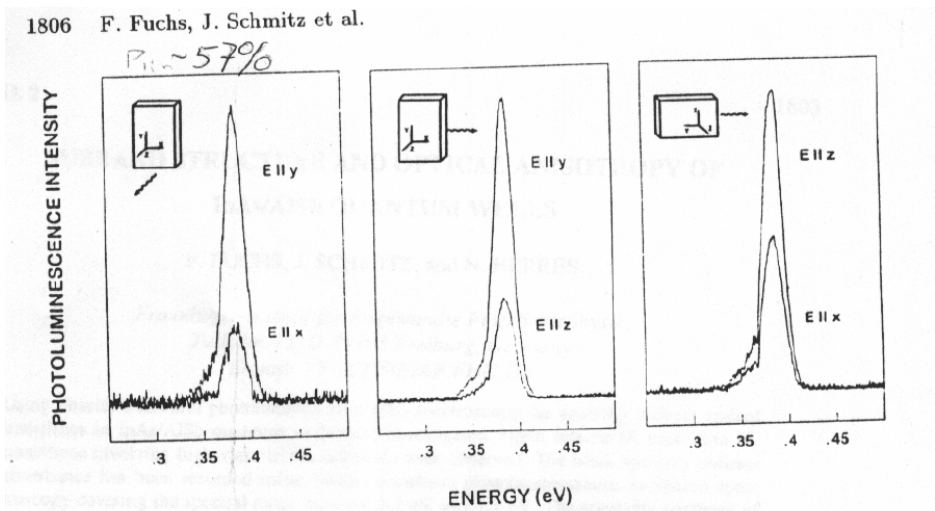

Fig. 3: Polarization-resolved PL of an InAs/AlSb double QW consisting of two 7.5-nm-wide InAs wells separated by a 5-nm-thick barrier. Left part shows emission with k parallel to the [100] growth direction z. The relative intensities are inverted upon exchange of the [011]-like emission directions x and y.

F. Fuchs, J. Schmitz and N. Herres,
Proc. the 23rd Internat. Conf. on Physics of Semiconductors,
vol. **3**, 1803 (Berlin, 1996)

Situation is typical for type-II heterostructures.
Here the anisotropy is ~ 60%

Tight-binding method: The main idea

$$\psi(\boldsymbol{r}) = \sum_{n,\alpha} C_n^{(\alpha)} \phi_{n\alpha}(x, y, z - z_n)$$

$$E_n^\alpha C_n^\alpha + \frac{1}{2} \sum_{n' \neq n, \alpha'} V_{n,n'}^{\alpha,\alpha'} C_{n'}^{\alpha'} = E C_n^\alpha$$

$$k_x = k_y = 0$$

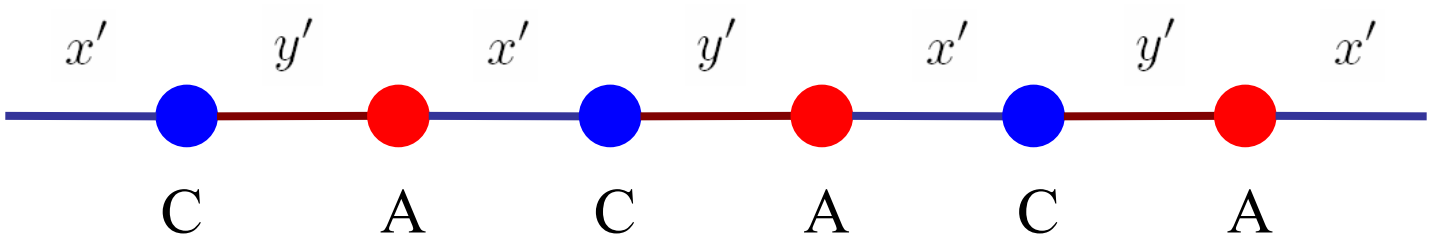

Tight-binding Hamiltonian

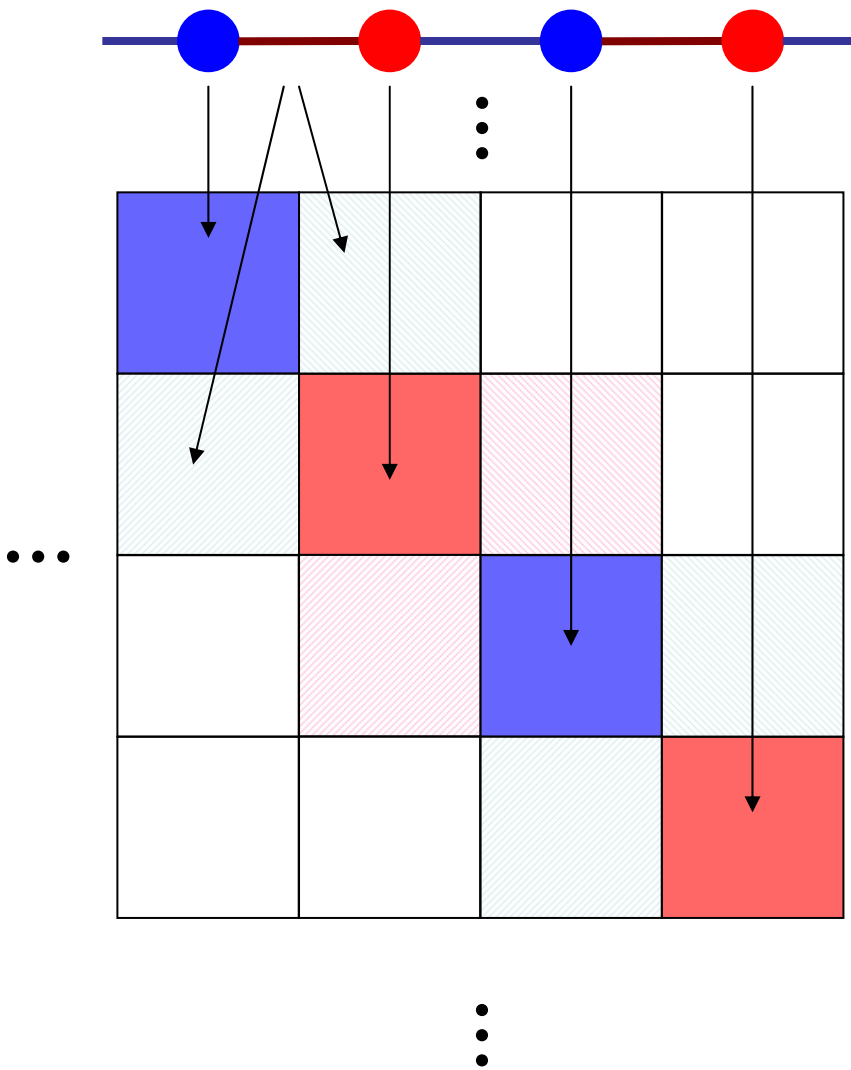

$$\hat{\mathcal{H}}\psi = E\psi$$

$$\hat{V}_{2l-1,2l-2}\hat{C}^{a}_{2l-2} + \left(\hat{E}_{2l-1} - E\right)\hat{C}^{c}_{2l-1} + \hat{V}_{2l-1,2l}\hat{C}^{a}_{2l} = 0$$

$$\hat{V}_{2l,2l-1}\hat{C}^{c}_{2l-1} + \left(\hat{E}_{2l} - E\right)\hat{C}^{a}_{2l} + \hat{V}_{2l,2l+1}\hat{C}^{c}_{2l+1} = 0$$

Optical matrix element

$$\hat{\boldsymbol{v}} = \frac{i}{\hbar}(\hat{\mathcal{H}}\boldsymbol{r} - \boldsymbol{r}\hat{\mathcal{H}}) \qquad v_{\alpha'\alpha}(\boldsymbol{R}', \boldsymbol{R}) = \frac{i}{\hbar}\,(\boldsymbol{R} - \boldsymbol{R}')\, H_{\alpha'\alpha}(\boldsymbol{R}', \boldsymbol{R})$$

$$\boldsymbol{M} = \langle \psi^e | \boldsymbol{v} | \psi^h \rangle \qquad P_{\text{lin}} = \frac{|M_x|^2 - |M_y|^2}{|M_x|^2 + |M_y|^2}$$

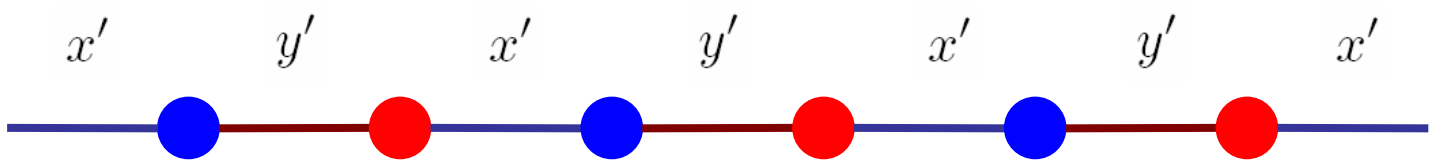

The choice of the parameters

sp3s* Tight-binding parameters for transport simulations in compound semiconductors

GERHARD KLIMECK†, R. CHRIS BOWEN
Jet Propulsion Laboratory, California Institute of Technology, Pasadena, CA 91109, U.S.A.

TIMOTHY B. BOYKIN
University of Alabama in Huntsville, Huntsville, AL 35899, U.S.A.

THOMAS A. CWIK
ECE Department and LICOS, Jet Propulsion Laboratory, California Institute of Technology, Pasadena, CA 91109, U.S.A.

(Received 25 February 2000)

A genetic algorithm approach is used to fit orbital interaction energies of sp3s* tight-binding models for the nine binary compound semiconductors consistent of Ga, Al, In and As, P, Sb at room temperature. The new parameters are optimized to reproduce the bandstructure relevant to carrier transport in the lowest conduction band and the highest three valence bands. The accuracy of the other bands is sacrificed for the better reproduction of the effective masses in the bands of interest. Relevant band edges are reproduced to within a few meV and the effective masses deviate from the experimental values typically by less than 10%.

Key words: sp3s* tight-binding, genetic algorithm, effective mass, parametrization, III–V material, GaAs, InAs, AlAs, GaP, InP, AlP, GaSb, InSb, AlSb.

Property	AlSb target	AlSb TB	InAs target	InAs TB
Γ_{6c}	2.300	2.300	0.370	0.368
Δ_{so}	0.673	0.675	0.380	0.381
m^*_Γ	0.120	0.121	0.024	0.024
$m^*_{lh}[001]$	−0.123	−0.099	−0.027	−0.028
$m^*_{lh}[011]$	−0.100	−0.089	−0.026	−0.027
$m^*_{lh}[111]$	−0.091	−0.086	−0.026	−0.027
$m^*_{hh}[001]$	−0.336	−0.363	−0.345	−0.364
$m^*_{hh}[011]$	−0.500	−0.632	−0.639	−0.657
$m^*_{hh}[111]$	−0.872	−0.800	−0.876	−0.883
m^*_{so}	−0.290	−0.196		−0.098
Δ_{min}	≈0.80	0.849		1.000
E^Δ_c	1.615	1.615	2.280	2.345
m^*_{Xl}	1.800	1.576		1.103
m^*_{Xt}	0.260	2.734		inf
L_{6c}	2.211	2.211	1.500	1.460
m^*_{Ll}		24.866		1.852
m^*_{Lt}		1.125		0.304
Γ_{6v}	-11.100	−10.975	-−12.300	−12.159 -
Γ_{7c}	3.740	5.075	4.390	4.126
Γ_{8c}	4.000	5.135	4.630	4.543
X_{5v}	−6.760	−6.995	−6.600	−7.595
X_{6v}	−3.000	−3.192	−2.400	−2.948
X_{7v}	−2.500	−2.858	−2.400	−2.836
X_{6c}	1.615	1.632	2.300	2.345
X_{7c}	3.020	2.614	2.500	2.849
L_{5v}	−6.250	−7.160	−6.230	−7.062
L_{6v}	−1.450	−1.613	−1.200	−1.399
L_{7v}	−1.000	−1.225	−0.900	−1.144
L_{7c}	4.400	3.476	5.400	3.713

The choice of the parameters

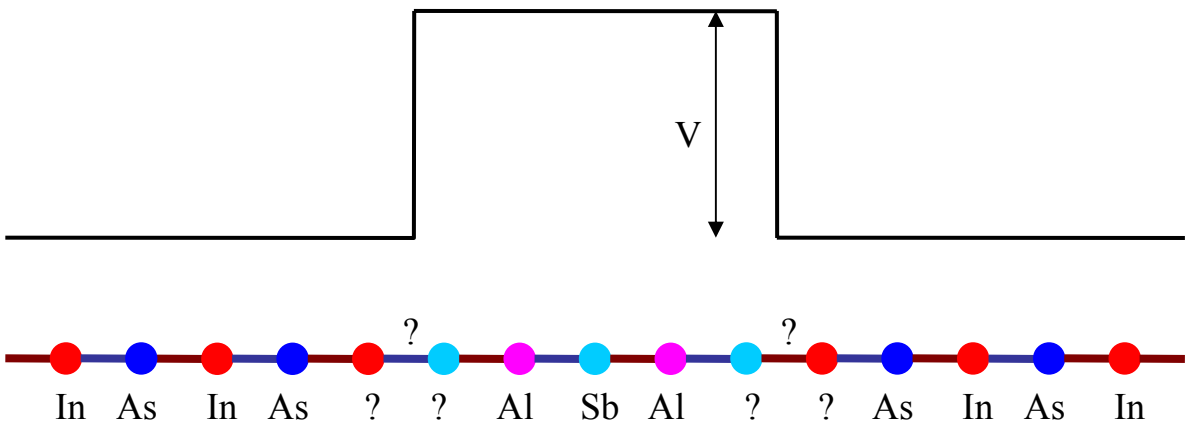

Electron states in thin QWs

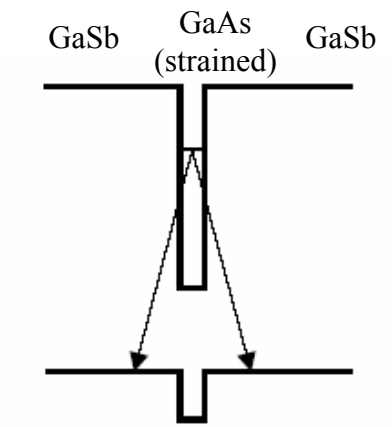

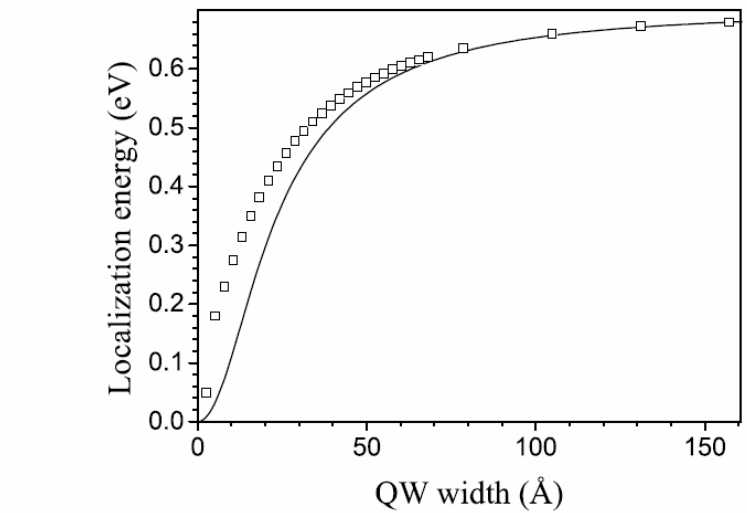

FIG. 10: Electron localization energy for a GaAs QW in a GaSb matrix. The solid curve represents the data obtained within the Kane model and open squares show the results of the tight-binding calculation.

A.A. Toropov, O.G. Lyublinskaya, B.Ya. Meltser,
V.A. Solov'ev, A.A. Sitnikova, M.O. Nestoklon, O.V. Rykhova,
S.V. Ivanov, K. Thonke and R. Sauer,
Phys. Rev B, submitted (2004)

Lateral optical anisotropy
Results of calculations

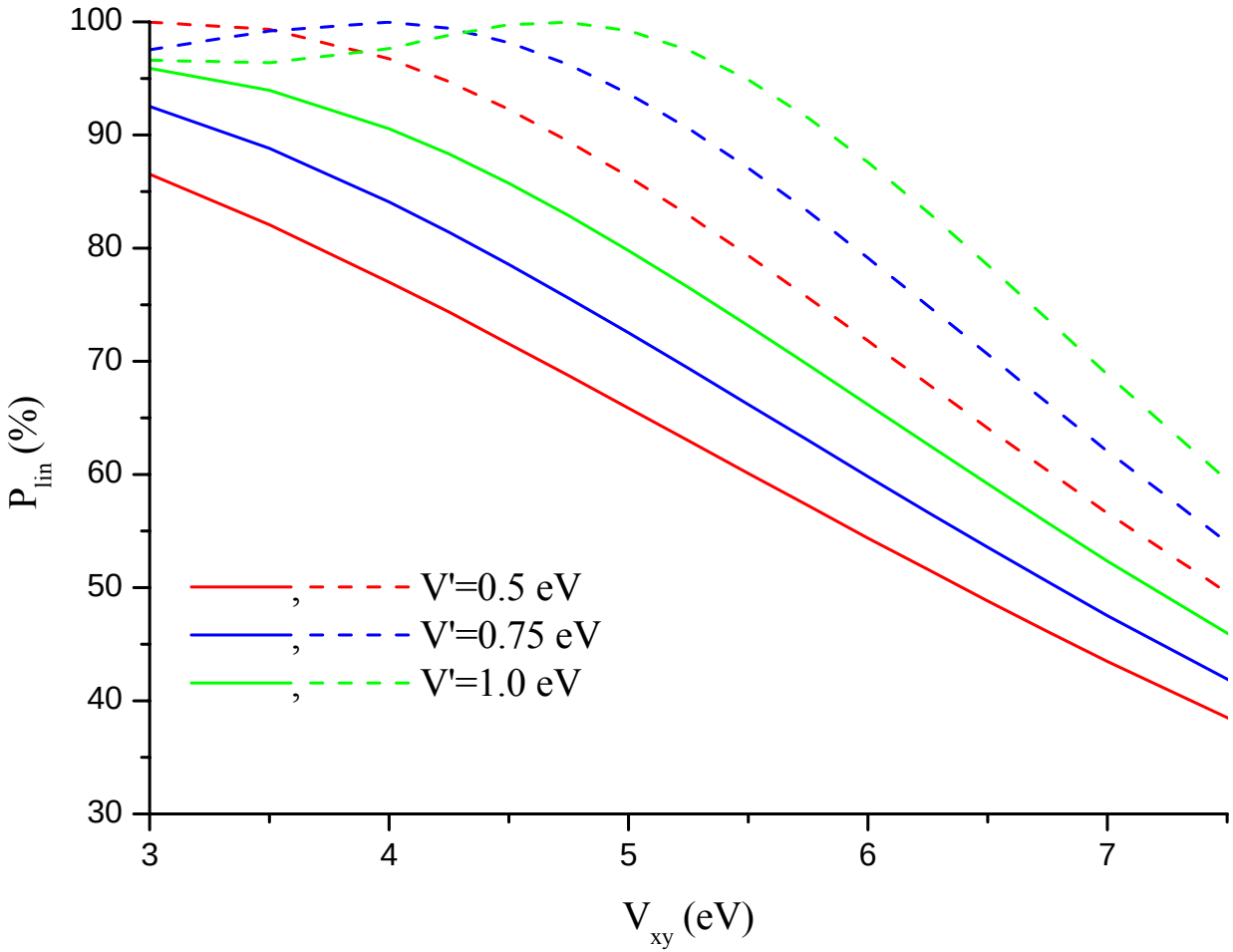

E.L. Ivchenko and M.O. Nestoklon, JETP **94**, 644 (2002);
arXiv http://arxiv.org/abs/cond-mat/0403297 (submitted to *Phys. Rev.* B)

Conclusion

- A tight-binding approach has been developed in order to calculate the electronic and optical properties of type-II heterostructures.
- the theory allows a giant in-plane linear polarization for the photoluminescence of type-II (001)-grown multi-layered structures, such as InAs/AlSb and ZnSe/BeTe.

Electron state in a thin QW

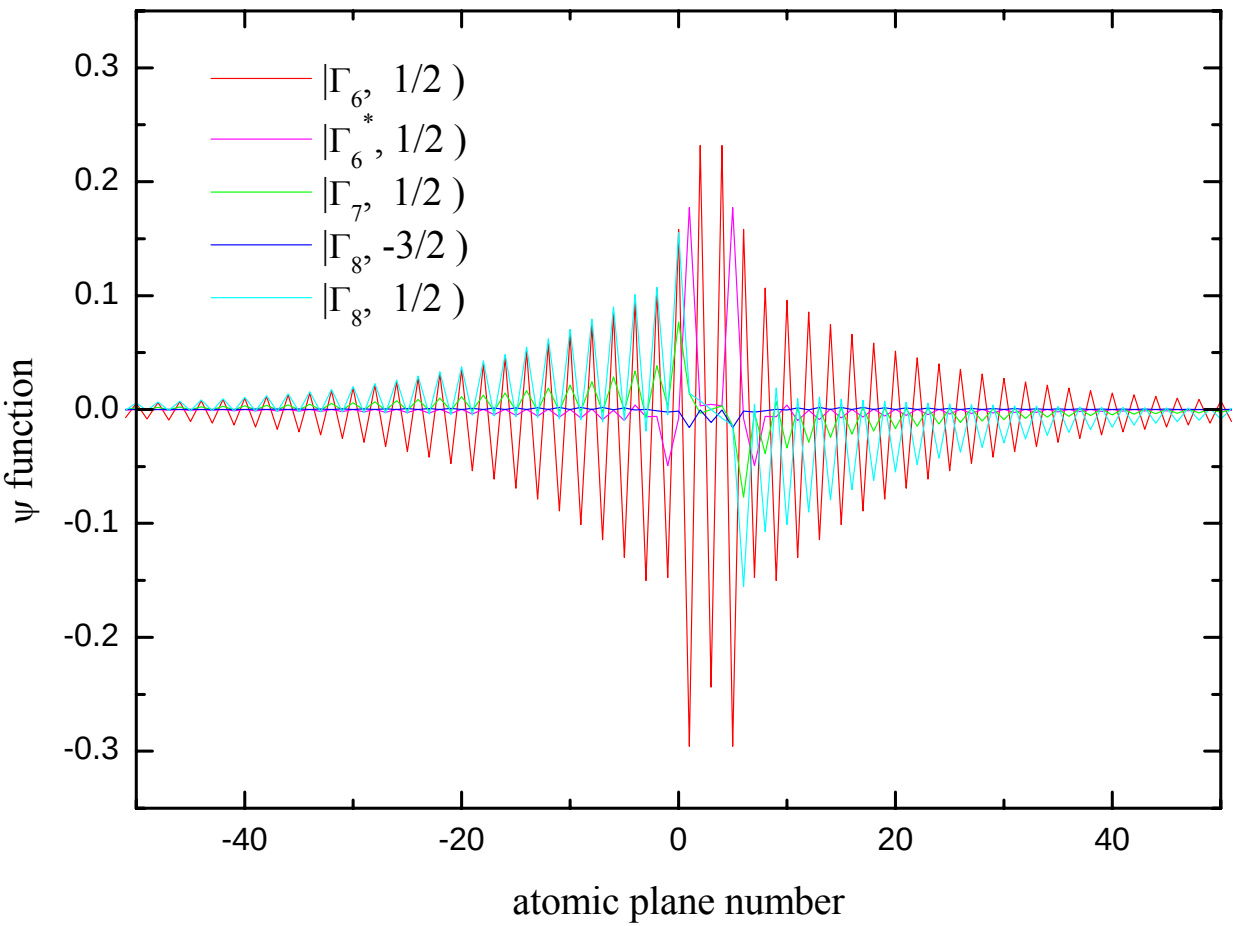

The main idea of the symmetry analysis

$$\hat{\mathcal{H}}\psi = E\psi$$

If crystal lattice has the symmetry transformations g
Then the Hamiltonian is invariant under these transformations:

$$\hat{\mathcal{D}}(g)\hat{\mathcal{H}}(g^{-1}\boldsymbol{r})\hat{\mathcal{D}}^{-1}(g) = \hat{\mathcal{H}}(\boldsymbol{r})$$

where $\hat{\mathcal{D}}(g)$ is point group representation

Time inversion symmetry

$$\mathcal{K}\psi = -i\hat{\sigma}_y\psi^*$$

$$\left|\pm\frac{1}{2}\right\rangle \rightarrow \left|\mp\frac{1}{2}\right\rangle$$

$$\left|\pm\frac{3}{2}\right\rangle \rightarrow \left|\mp\frac{3}{2}\right\rangle$$

Basis functions

- Для описания экспериментальных данных необходим
  - учёт спин-орбитального расщепления валентной зоны
  - для описания непрямозонных полупроводников “верхние орбитали” (s*)

$$|\Gamma_6, 1/2\rangle = \uparrow S\,, \qquad |\Gamma_6, -1/2\rangle = \downarrow S\,,$$

$$|\Gamma_8, -3/2\rangle = \downarrow \frac{X - \mathrm{i}Y}{\sqrt{2}}\,, \qquad |\Gamma_8, 3/2\rangle = -\uparrow \frac{X + \mathrm{i}Y}{\sqrt{2}}\,,$$

$$|\Gamma_8, 1/2\rangle = \sqrt{\frac{2}{3}}\uparrow Z - \downarrow \frac{X + \mathrm{i}Y}{\sqrt{6}}\,, \qquad |\Gamma_8, -1/2\rangle = \sqrt{\frac{2}{3}}\downarrow Z + \uparrow \frac{X - \mathrm{i}Y}{\sqrt{6}}\,,$$

$$|\Gamma_7, 1/2\rangle = \frac{1}{\sqrt{3}}[\uparrow Z + \downarrow (X + \mathrm{i}Y)]\,, \qquad |\Gamma_7, -1/2\rangle = \frac{1}{\sqrt{3}}[\downarrow Z - \uparrow (X - \mathrm{i}Y)]\,,$$

$$|\Gamma_6^*, 1/2\rangle = \uparrow S^*\,, \qquad |\Gamma_6^*, -1/2\rangle = \downarrow S^*\,,$$

~ 20-зонная модель. 15 параметров

Hamiltonian matrix elements

$$\hat{E}_b = \frac{1}{2}\begin{bmatrix} E_{sb} & 0 & 0 & 0 & 0 \\ 0 & E_{pb}+\frac{1}{3}\Delta_b & 0 & 0 & 0 \\ 0 & 0 & E_{pb}+\frac{1}{3}\Delta_b & 0 & 0 \\ 0 & 0 & 0 & E_{pb}-\frac{2}{3}\Delta_b & 0 \\ 0 & 0 & 0 & 0 & E_{s^*b} \end{bmatrix}$$

$$\hat{V}_{2l-1,2l} = \frac{1}{2}\begin{bmatrix} V_{ss} & 0 & \eta V_{sc,pa} & \xi V_{sc,pa} & 0 \\ 0 & V_{xx} & -\xi V_{xy} & \eta V_{xy} & 0 \\ -\eta V_{sa,pc} & -\xi V_{xy} & V_{xx} & 0 & -\eta V_{s^*a,pc} \\ -\xi V_{sa,pc} & \eta V_{xy} & 0 & V_{xx} & -\xi V_{s^*a,pc} \\ 0 & 0 & \eta V_{s^*c,pa} & \xi V_{s^*c,pa} & 0 \end{bmatrix}$$

where $\eta = \sqrt{2/3}$, $\xi = \sqrt{1/3}$.

$$\{\hat{V}_{2l-1,2l-2}\}_{\alpha,\alpha'} = (1-2\delta_{\alpha,\alpha'})\{\hat{V}_{2l-1,2l}\}_{\alpha,\alpha'} ,$$
$$\{\hat{V}_{2l,2l-1}\}_{\alpha,\alpha'} = \{\hat{V}_{2l-1,2l}\}_{\alpha',\alpha} ,$$
$$\{\hat{V}_{2l,2l+1}\}_{\alpha,\alpha'} = (1-2\delta_{\alpha,\alpha'})\{\hat{V}_{2l-1,2l}\}_{\alpha',\alpha} .$$

Optical matrix elements

$$V_l^x = \hat{C}_{2l-1}^{c,A\dagger}\hat{V}_{x1}\hat{C}_{2l}^{v,B} + \hat{C}_{2l}^{c,A\dagger}\hat{V}_{x2}\hat{C}_{2l-1}^{v,B}\,,$$
$$V_l^y = \hat{C}_{2l+1}^{e,A\dagger}\hat{V}_{y1}\hat{C}_{2l}^{v,B} + \hat{C}_{2l}^{e,A\dagger}\hat{V}_{y2}\hat{C}_{2l+1}^{v,B}\,.$$

$$\hat{V}_{x1} = \frac{1}{\sqrt{2}}\begin{bmatrix} 0 & -V_{sc,pa} & \xi V_{sc,pa} & -\eta V_{sc,pa} & 0 \\ -V_{sa,pc} & 0 & \eta V_{xy} & \xi V_{xy} & -V_{s^*a,pc} \\ \xi V_{sa,pc} & -\eta V_{xy} & 0 & -V_{xy} & \xi V_{s^*a,pc} \\ -\eta V_{sa,pc} & -\xi V_{xy} & V_{xy} & 0 & -\eta V_{s^*a,pc} \\ 0 & -V_{s^*c,pa} & \xi V_{s^*c,pa} & -\eta V_{s^*c,pa} & 0 \end{bmatrix}$$

$$\hat{V}_{y1} = \frac{\mathrm{i}}{\sqrt{2}}\begin{bmatrix} 0 & -V_{sc,pa} & -\xi V_{sc,pa} & \eta V_{sc,pa} & 0 \\ -V_{sa,pc} & 0 & -\eta V_{xy} & -\xi V_{xy} & -V_{s^*a,pc} \\ -\xi V_{sa,pc} & \eta V_{xy} & 0 & -V_{xy} & -\xi V_{s^*a,pc} \\ \eta V_{sa,pc} & \xi V_{xy} & V_{xy} & 0 & \eta V_{s^*a,pc} \\ 0 & -V_{s^*c,pa} & -\xi V_{s^*c,pa} & \eta V_{s^*c,pa} & 0 \end{bmatrix}$$

$$\hat{V}_{x2} = \tilde{\hat{V}}_{x1},\ \hat{V}_{y2} = \tilde{\hat{V}}_{y1}$$